Nonlinear effects in seismic base isolations

DINU BRATOSIN
Department of Dynamic Systems
Institute of Solid Mechanics of the Romanian Academy
C-tin Mille Street, No.15, 10141 Bucharest 1
ROMANIA
E-mail: bratosin@acad.ro

Abstract: - By interposing a layer with low horizontal stiffness but with high damping characteristics between the structure and his foundation, an aseismic isolation system partly decouples the building structure from the horizontal components of the earthquake ground motion and thus diminishes the structural demand.

As a result of the lateral flexibilization, the natural period of the former fixed-base structure undergoes a jump and the new base-isolation structure has a new and larger natural period. This "period-shift" can extract a structure away from the dominant period of the earthquake ground motion and thus can avoid the destructive effects given by the system resonance.

The dynamic behavior of the materials and devices of the isolating layer governs the performance of base-isolation system. The dynamic properties, such as horizontal stiffness and damping capacity determine the filtering role of the isolating layer and, finally, the structural dynamic response. But all of materials and devices used in an isolating layer systems exhibit, more or less, a nonlinear behavior. In addition, all site soils materials have the well-known nonlinear mechanical characteristics, which affect the dynamic structural response. Thus, in the dynamic response evaluation of a base-isolated system the nonlinear behavior of both isolator and site layers must taken into account.

This paper presents a method for the necessary period-shift determination by using the dynamic linear or/and nonlinear magnification functions. For the nonlinear magnification functions determination we shall use a nonlinear Kelvin-Voigt model (NKV model) for base-isolated structure, which is able to model the effects of the soils and isolating layer nonlinearity on the shape and resonant magnitude of the magnification functions. Thus, we shall obtain a proper tool for modeling the resonant peak dispersion, which is a very important condition for a correct period-shift evaluation and therefore for a correct isolation design.

Key-Words: - Earthquake engineering, Nonlinear dynamics, Seismic base-isolation

1 Introduction

Passive base isolation systems are one of the most successful and widely implemented technologies for seismic hazard mitigation. In the last decade several base isolation systems have developed for seismic protection of the structure with the special destinations as hospitals, emergency communication centers, fire stations, traffic management centers, bridges, historical buildings, etc. [10], [14], [17]. The performance of the base isolated buildings in different parts of the world during earthquakes in the recent past established that the base isolated technology is a viable alternative to the conventional earthquake resistant design of a large category of buildings.

In the past decades, the field of dynamics behaviour of the base-isolated systems has received a lot of attention. An increasing amount of papers have been dedicated to several theoretical and experimental aspects [1-3], [6-9], [12-13], [16], [18], [20-24].

Although it is well-known that these isolation systems may exhibit nonlinear behavior, they are often linearly modeled in engineering practice, as prescribed in some building codes. But, this linear assumption can lead to an unrealistic representation of the dynamic response.

The fundamental concept of the base isolation systems is to partly uncouple the building structures from the damaging components of the earthquake input motion by introducing a flexible interface between the structure and his foundation. Thus, one can limit the amount of forces that are transferred to the superstructure and the structural demand can be diminished.

However, this excellent strategy is not suitable for all buildings and for all emplacements.

In terms of structure and site natural periods and in terms of correct period-shift evaluation, this

positive period-shift can extract the structure away from the characteristic period contents of earthquake ground motions or, contrary, can throw the structural ensemble into resonant conditions.

Because the first condition (connected from structural and site natural periods) is self-evident, there will be further presented some remarks regarding the nonlinear effects given by mechanical properties of the isolated and site layers upon the correct period-shift evaluation.

We shall focus on two main objectives. The first is to present a method for the necessary period-shift determination based on linear and/or nonlinear magnification functions and the second objective is to evaluate the effects of the nonlinear behavior on the shape and amount of the magnification functions.

In a base-isolated structural system, the large differences between mechanical characteristics of the structural materials and isolator materials allow us to treat the base-isolated system as a two-degree-of-freedom system (2dof system), see [7], [11], [16]. Accepting this hypothesis, in chapter 2 we will present such a 2dof system. Using this 2dof model one can prove that the first fundamental frequency of the base isolated buildings is close to the frequency of the sdof system constituted by rigid superstructures mounted on flexible base isolators. Therefore, the isolated building tends to behave globally as a rigid body and all the deformability processes are located at the isolating layer.

Accepting these approximations and considering the linear behavior of the isolating layer, in chapter 3 such a linear sdof model (Kelvin-Voigt model) is used for giving a first estimation of necessary period-shift. In this aim, we shall use the magnification function ability to illustrate the resonance behavior, see also [7], [11].

However, the real behavior of the isolating layer is a nonlinear one. Thus, for a correct assessment of the period-shift amount a nonlinear sdof model is needed. For this reason, in chapter 4 a nonlinear sdof model obtained by the extension of the linear Kelvin-Voigt model in nonlinear domain will be presented, see [4], [5], [6]. This nonlinear Kelvin-Voigt model (NKV model) is able to describe the essential characteristics of the dynamic nonlinear behavior – the strain dependency and hysteretic damping capacity. In addition, the NKV model is suitable to the equivalent linearization process.

Using the NKV model, in chapter 5 we will present the effects given by the nonlinear properties of the isolating layer. The dispersion of the nonlinear magnification function peaks proves that the linear estimation of the necessary period-shift must be corrected, [7].

Finally, chapter 6 contains some remarks on soils nonlinearity effects. Based on experimental data and numerical simulation, the enlargement tendency of the period-shift is pointed out, [4], [7].

2 Two-degree-of-freedom model for base-isolated structure

Let us consider a structure isolated from its base by a certain isolation system.

Due to large differences between mechanical characteristics of the structural and isolator materials, a two-degree-of-freedom (2dof) simplified model can be used to predict the dynamic response of such a base isolated structure (Fig. 1) [7], [16].

The superstructure is assimilated to a single degree of freedom (sdof) system (characterized by the mass m_s, damping c_s and stiffness k_s) mounted on the base assimilated to another sdof system (characterized by the mass m_b, damping c_b and stiffness k_b).

If x_g, x_b and x_s are the ground, base and superstructure absolute displacements, the base and superstructure displacements relative to the ground are:

$$u_b = x_b - x_g \quad ; \quad u_s = x_s - x_g . \tag{1}$$

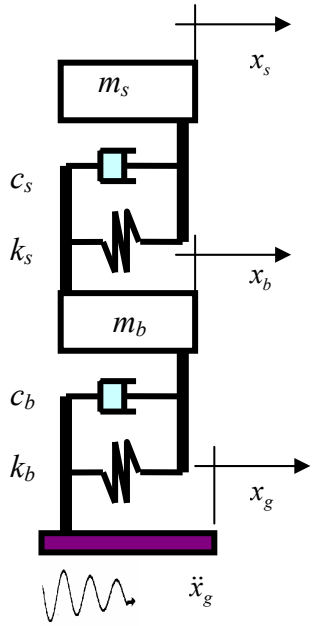

Fig.1 2dof model for a base-isolated structure

The motion equations for this 2dof system are:

$$\begin{cases} m_b\ddot{x}_b + m_s\ddot{x}_s + c_b\left(\dot{x}_b - \dot{x}_g\right) + k_b\left(x_b - x_g\right) = 0 \\ m_s\ddot{x}_s + c_s\left(\dot{x}_s - \dot{x}_b\right) + k_s\left(x_s - x_b\right) = 0 \end{cases} \quad (2)$$

where the $\dot{x}$ denotes the time derivative.

Since

$$x_b = u_b + x_g \quad ; \quad x_s = u_s + u_b + x_g \quad (3)$$

the system (2) becomes:

$$\begin{cases} m_b\ddot{u}_b + m_s\left(\ddot{u}_s + \ddot{u}_b\right) + c_b\dot{u}_b + k_b u_b = -\left(m_b + m_s\right)\ddot{x}_g \\ m_s\left(\ddot{u}_s + \ddot{u}_b\right) + c_s\dot{u}_s + k_s u_s = -m_s\ddot{x}_g \end{cases} \quad (4)$$

or, in matricial form:

$$\mathbf{M}\ddot{\mathbf{x}} + \mathbf{C}\dot{\mathbf{x}} + \mathbf{K}\mathbf{x} = -\mathbf{M}\boldsymbol{\delta}\ddot{x}_g \quad (5)$$

where the mass, damping and stiffness matrices are, respectively:

$$\mathbf{M} = \begin{bmatrix} m_s + m_b & m_s \\ m_s & m_s \end{bmatrix} \; ; \; \mathbf{C} = \begin{bmatrix} c_b & 0 \\ 0 & c_s \end{bmatrix} \; ; \; \mathbf{K} = \begin{bmatrix} k_b & 0 \\ 0 & k_s \end{bmatrix} \quad (6)$$

$\boldsymbol{\delta}$ is a position vector: $\boldsymbol{\delta} = \{1 \quad 0\}^T$, $\mathbf{x}$ is the displacement vector $\mathbf{x} = \{u_b \quad u_s\}^T$ and $\dot{\mathbf{x}}$, $\ddot{\mathbf{x}}$ denotes the time derivatives of the displacement vector.

Assuming the structure together with its base as a perfectly rigid body mounted on isolators, a single degree of freedom model with the circular frequency results

$$\omega_b^2 = \frac{k_b}{m_t} \quad (7)$$

where m_t is the total mass: $m_t = m_b + m_s$.

Also, assuming the structure with fixed base another sdof system result, with the circular frequency:

$$\omega_s^2 = \frac{k_s}{m_s} \quad (8)$$

By introducing the frequential ratio:

$$\varepsilon = \frac{\omega_b^2}{\omega_s^2} \quad (9)$$

and the mass ratio:

$$\mu = \frac{m_b}{m_s} \quad (10)$$

the dynamic matrix $\mathbf{D} = \mathbf{K} - p^2\mathbf{M}$ becomes:

$$\mathbf{D} = \omega_s^2\begin{bmatrix} \varepsilon\dfrac{1+\mu}{\mu} & -\dfrac{1}{\mu} \\ -\varepsilon\dfrac{1+\mu}{\mu} & \dfrac{1+\mu}{\mu} \end{bmatrix} \quad (11)$$

The fundamental frequencies of 2dof system result now as the eigenvalues of the dynamic matrix in the form:

$$p_{1,2}^2 = \frac{\omega_s^2}{2}\begin{bmatrix} \dfrac{(\mu+1)(\varepsilon+1)}{\mu} \mp \\ \mp\dfrac{(\mu+1)(\varepsilon-1)}{\mu}\sqrt{1+\dfrac{4\varepsilon}{(\mu+1)(\varepsilon-1)^2}} \end{bmatrix} \quad (12)$$

By developing the term under the square root in a binomial series, the fundamental frequencies of the 2dof system become

$$\begin{aligned} p_1^2 &\cong \omega_s^2\frac{\varepsilon}{\varepsilon+1} = \omega_b^2\frac{1}{\varepsilon+1} \\ p_2^2 &\cong \omega_s^2\frac{(\mu+1)(\varepsilon+1)}{\mu} \end{aligned}, \quad (13)$$

see [21], and the normalized form of the fundamental modes are:

$$\mathbf{X}_1 = \{1 \quad \varepsilon+1\}^T \quad ; \quad \mathbf{X}_2 = \left\{1 \quad -\frac{\mu}{\varepsilon+1}\right\}^T. \quad (14)$$

Since $\omega_s << \omega_b$ the frequential ratio ε has small values. In these conditions, the first fundamental frequency of the 2dof model is given in a large proportion by the isolating layer frequency $p_1 \cong \omega_b$. This means that the first fundamental frequency of the base isolating building is close to the frequency of the sdof system constituted by rigid superstructure mounted on a flexible base isolator and the isolated building tends to behave globally as an sdof system.

The modal participation factors are, [14]:

$$L_i = \frac{\mathbf{X}_i^T\mathbf{M}\boldsymbol{\delta}}{\mathbf{X}_i^T\mathbf{M}\mathbf{X}_i} \quad (15)$$

thus, by the replacement of the appropriate fundamental modes values (14) are

$$L_1 = \frac{\mu + (\varepsilon+1)}{\mu + (\varepsilon+1)^2} \quad ; \quad L_2 = \frac{\varepsilon(\varepsilon+1)}{\mu + (\varepsilon+1)^2} \quad (16)$$

and by a series development they become:

$$L_1 = 1 - \frac{\varepsilon}{\mu+1} \cong 1 \quad ; \quad L_2 = \frac{\varepsilon}{\mu+1} << 1. \quad (17)$$

These relations show that the participation factor for the first mode approaches the unity, which

means the sdof behavior too. The participation factor for the second mode is very small, therefore even if the second fundamental frequency p_2 is within the range of high spectral acceleration, the smallness of the participation factor ensures that the second mode is not highly excited by the ground motion.

In these conditions, the quasi-rigid structural behavior hypothesis becomes acceptable and the 2dof system can be reduced to an sdof system where the dynamic behavior is governed by isolated layer characteristics (Fig.2).

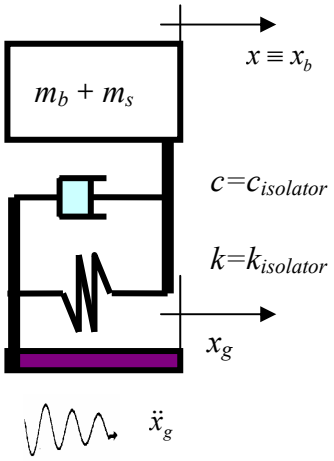

Fig. 2 A simplified model for a base-isolated structure

3 Linear assessment of necessary period-shift

For a qualitative evaluation of the necessary period-shift value, one can consider the structure with fixed base as a linear sdof subjected to harmonic abutment accelerations (Fig. 2):

$$\ddot{x}_g(t) = \ddot{x}_g^0 \sin \omega t \tag{18}$$

where $\ddot{x}_g^0$ is the acceleration amplitude (usually connected by peak ground accelerations - *PGA*) and ω is the pulsation of the excitation.

In linear dynamics, a usual description of such sdof behavior is given by the linear Kelvin-Voigt model consisting of a mass *m* supported by a spring (with a stiffness *k*) and a dashpot (with a viscosity *c*) connected in parallel. The governing equation of the KV system is :

$$m\ddot{x} + c \cdot \dot{x} + k \cdot x = -m\ddot{x}_g^0 \tag{19}$$

see [11], or:

$$\ddot{x} + 2\zeta\omega_0\dot{x} + \omega_0^2 x = -\omega_0^2 \ddot{x}_g^0 \tag{20}$$

where ω_0 is undamped natural pulsation and ζ is the damping ratio:

$$\omega_0 = \sqrt{\frac{k}{m}} \quad ; \quad \zeta = \frac{c}{c_{cr}} = \frac{c}{2m\omega_0} \tag{21}$$

By using the change of variable $\tau = \omega_0 t$ and by introducing a new "time" function

$$\varphi(\tau) = x(t) = x\left(\frac{\tau}{\omega_0}\right)$$

as in [5], one can obtain by eq. (20) a dimensionless form of the equation of motion:

$$\varphi'' + C\varphi' + K\varphi = \mu \sin \upsilon\tau \tag{22}$$

where φ' denotes the time derivative with respect to τ and:

$$C = \frac{c}{m\omega_0} = 2\zeta \quad ; \quad K = \frac{k}{m\omega_0^2} = 1$$
$$\mu = \frac{\ddot{x}_g^0}{\omega_0^2} \quad ; \quad \upsilon = \frac{\omega}{\omega_0} \tag{23}$$

The steady-state solution of the equation (22) can be written as:

$$\varphi(\tau, \upsilon, \zeta) = \mu\Phi(\upsilon;\zeta)\sin(\upsilon\tau - \psi) \tag{24}$$

where $\Phi(\upsilon;\zeta)$ is *the magnification function:*

$$\Phi(\upsilon;\zeta) = \frac{\max_\tau\left[\varphi(\tau,\upsilon,\zeta)\right]}{\mu} = \frac{x_{dynamic}}{x_{static}}$$

a ratio of maximum dynamic amplitude $\varphi_{\max} \equiv x_{dynamic}$ to static displacement $\mu = x_{static}$. The analytical expression of this magnification function is:

$$\Phi(\upsilon;\zeta) = \frac{1}{\sqrt{\left(1-\upsilon^2\right)^2 + \left(2\zeta\upsilon\right)^2}} \tag{25}$$

Usually, in the structural dynamics one uses the periods T instead of the pulsations ω. Because $T = 2\pi/\omega$ and $\upsilon = \omega/\omega_0 = T_0/T$, the magnification function in terms of period becomes:

$$\Phi(T;T_0,\zeta) = \frac{1}{\sqrt{\left[1-\left(\frac{T_0}{T}\right)^2\right]^2 + \left[2\zeta\left(\frac{T_0}{T}\right)\right]^2}} \tag{26}$$

The magnification function in terms of dimensionless pulsation υ, (25) or period T ,(26) for a system with $\omega_0 = 21$ rad/s $\Rightarrow$ $T_0 = 0.3$ s and $\zeta = ct.$ has typical aspects as there are depicted in Fig. 3.

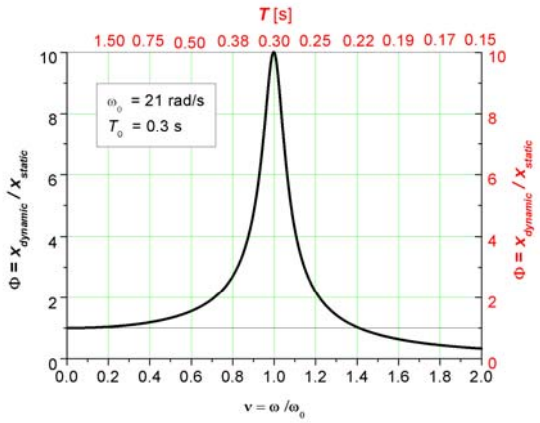

Fig. 3 The magnification function

Now we can use the magnification function to illustrate the structural behavior before and after period jump, that is to illustrate the behavior differences between a structure with fixed base and the same structure but with an isolating layer.

In order to exemplify the ability of the magnification functions to illustrate the resonant behavior of the base-isolated structure in the next we will present a comparative study of a structure with and without a base isolation.

Let us consider the structure with the following mechanical characteristics [20]:

$$m_s = 30000 \text{ kg} \;;\; T_s = 0.3 \text{ s} \;;\; \zeta = 0.5\%. \qquad (27)$$

We assume that such a structure is located on a usual site, composed, for example, by rocks or consolidated aluvionary deposits with $T_0 = 0.3 \div 0.4$ s. In these conditions, this structure becomes a proper candidate for isolated base technology.

As one can see in Fig.4, a small period-shift from the resonant period of 0.3 s up to the base-isolated period of 0.5 s takes out the structure from the dangerous resonant zone and leads to a great reduction of the dynamic magnification amount.

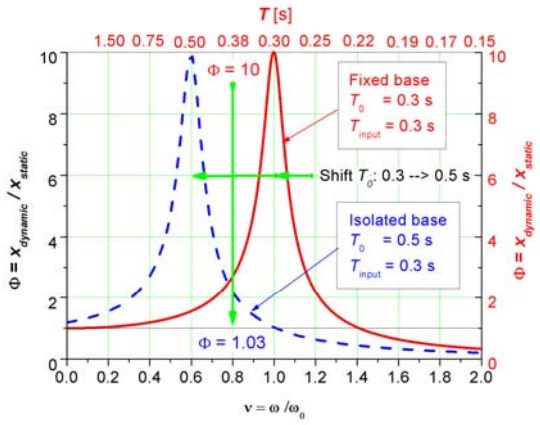

Fig. 4 A period-shift example

4 Nonlinear Kelvin-Voigt model

4.1 Nonlinear extending

As we have seen in chapter 2, the mechanical characteristics of the isolated layer govern the dynamic response of the sdof model for base-isolated structures. The experimental tests prove that all materials and devices used in isolated layers exhibit, more or less, a nonlinear behavior. Therefore, the sdof system of a base-isolated structure must be a nonlinear one.

Using the same method that describes the nonlinearity by strain or displacement dependence of the material parameters, we assume that the damper viscosity c and the spring stiffness k are functions of the displacement x, [4], [6]:

$$c = c(x) \quad ; \quad k = k(x). \qquad (28)$$

Using these dynamic material functions, $c(x)$ and $k(x)$, the differential equation of the nonlinear sdof system can be written as an extension of eq. (19):

$$m\ddot{x} + c(x)\cdot\dot{x} + k(x)\cdot x = -m\ddot{x}_g \qquad (29)$$

or by extension of the eq. (20):

$$\ddot{x} + 2\omega_0\zeta(x)\cdot\dot{x} + \omega_0^2 k_n(x)\cdot x = -\ddot{x}_g. \qquad (30)$$

Using the same change of variable $\tau = \omega_0 t$ and the "time" function $\varphi(\tau) = x(t) = x(\tau/\omega_0)$ one obtains for eq. (29) or eq. (30) another form:

$$\varphi'' + C(\varphi)\cdot\varphi' + K(\varphi)\cdot\varphi = \mu\sin\upsilon\tau \qquad (31)$$

where

$$\varphi'(\tau) = \frac{\partial\varphi}{\partial\tau} = \frac{1}{\omega_0}\dot{x} \quad ; \quad \varphi''(\tau) = \frac{\partial^2\varphi}{\partial\tau^2} = \frac{1}{\omega_0^2}\ddot{x} \qquad (32)$$

and

$$C(\varphi) \equiv C(x) = \frac{c(x)}{m\omega_0} = 2\zeta(x)$$
$$K(\varphi) \equiv K(x) = \frac{k(x)}{m\omega_0^2} = \frac{k(x)}{k(0)} = k_n(x) \qquad (33)$$

The transformed amplitude μ and the normalized pulsation υ remain in the same linear form:

$$\mu = -\frac{\ddot{x}_g^0}{\omega_0^2} \quad ; \quad \upsilon = \frac{\omega}{\omega_0}. \qquad (34)$$

The solution of the equation (31) can be written like as eq. (24):

$$\varphi(\tau,\upsilon,\mu)=\mu\Phi(\upsilon,\mu)\sin(\upsilon\tau-\psi) \qquad (35)$$

Thus, in this nonlinear case, the solution $\varphi(\tau,\upsilon,\mu)$ and the magnification function $\Phi(\upsilon,\mu)$ become dependent on the load through the transformed amplitude μ.

For a given amplitude μ and a relative pulsation υ, the nonlinear equation (31) can be numerically solved using a computer program [5] based on Newmark algorithm [15]. After this, using a known solution and a known excitation, the nonlinear magnification function was obtained first in term of normalized pulsation υ and after then in terms of period:

$$\Phi(\upsilon)=\Phi(\upsilon,\mu)\Big|_{\substack{\mu=ct.\\ \omega_0=ct.}} \quad \Rightarrow \quad \Phi(T)\Big|_{\substack{\mu=ct.\\ T_0=ct.}} \qquad (36)$$

like as in the example in Fig.5, where some nonlinear magnification functions for rubber are presented.

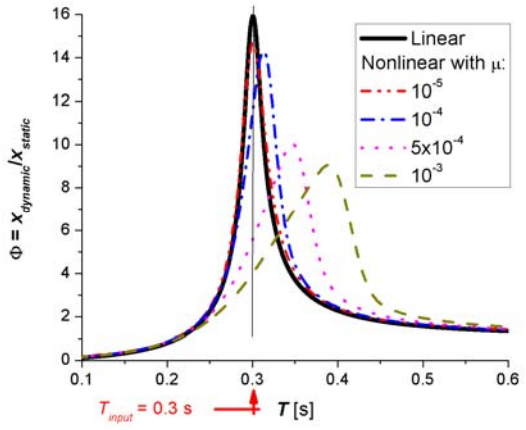

Fig. 5 Typical non-linear magnification functions (resonant column test with rubber sample)

We can see in Fig. 5 that the peak amplitudes of the nonlinear magnification functions depend on the excitation amplitude, have a decreasing resonant amount and occur at different periods situated after the linear resonant period. In this example where a material with softening stiffness was tested, the resonant peaks are displaced towards long periods. But, the experimental tests upon materials or devices with the hardening stiffness show peak displacements towards short periods [6], [11], [18] .

Such a peak dispersion has been already met at isolator materials or devices used for base-isolated structures [6], [11]. This nonlinear behavior affects the entire response of the base isolated system, including the period-shift determination [7] .

4.2 Hysteretic damping modeling

The definition and utilization of the nonlinear Kelvin-Voigt model are based on the equivalence hypothesis between the hysteretic and viscous material damping [4]. For this reason, it is necessary to verify the capabilities of this viscoelastic model to describe the hysteretic damping.

Several methods use the experimental registered hysteretic loops for the damping evaluation and determine the damping ratio as:

$$\zeta=\frac{1}{4\pi}\frac{\Delta W}{W} \qquad (37)$$

where W is the maximum stored energy and ΔW is the energy loose per cycle represented by the area enclosed inside the hysteresis loop (Fig. 6) [5], [11].

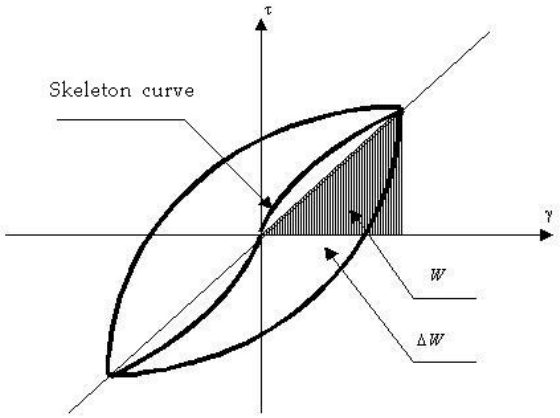

Fig. 6 Damping evaluation from hysteresis loop

By another method, the hysteretic loop is built from the skeleton curve by applying the Masing rule that postulates that the superior and inferior branches can be obtained from the skeleton curve by multiplying by a factor 2 in both directions [11].

To verify the capabilities of the non-linear Kelvin-Voigt equation (31) to model a hysteretic loop we will use an inverse path. Starting from given dynamic material functions of the NKV model we can build the hysteretic loops for a certain deformation levels. Then, the damping ratio value ζ for a certain deformation level will be obtained with a hysteretic method and compared with the experimental value at the same deformation level, [5].

We will illustrate this method using the material function obtained from torsional resonant column test performed upon rubber sample (Fig.7).

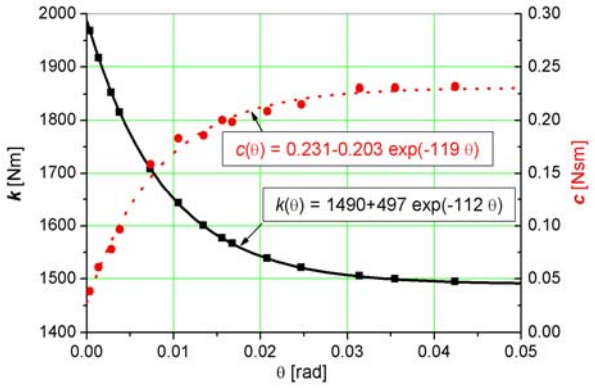

Fig. 7 Torsional material function of a rubber sample

The restoring force of the nonlinear Kelvin-Voigt torsional model is:

$$Q(\theta,\dot{\theta}) = Q_{el}(\theta) + Q_{dam}(\theta,\dot{\theta}) = k(\theta)\cdot\theta + c(\theta)\cdot\dot{\theta} \tag{38}$$

where $Q_{el}(\theta) = k(\theta)\cdot\theta$ is the skeleton curve equation.

For a certain amount of the excitation $M = M_0 \sin\omega t$ the displacement response θ (after the dropping the transitory part) has the form:

$$\theta = \theta_0 \cos\omega t\,, \tag{39}$$

and, then:

$$\dot{\theta} = \theta_0 \omega \sin\omega t\,. \tag{40}$$

Therefore, by eliminating the time t between this two equations, (39) and (40), it follows:

$$\dot{\theta} = \pm\omega\sqrt{\theta_0^2 - \theta}\,, \tag{41}$$

and the restoring force (38) becomes:

$$Q(\theta) = k(\theta)\cdot\theta \pm c(\theta)\cdot\omega\sqrt{\theta_0^2 - \theta}\,, \tag{42}$$

where the sign "+" is for the superior branch of the hysteretic loop and the sign "-" for the inferior branch.

For the deformation level $\theta_0 = 2.076$ % the hysteretic loop given by eq. (42) is illustrated in Fig. 8.

For comparison, the Masing hysteretic loop for the same tested rubber, at the same amplitude level, built using the same skeleton curve $Q_{el}(\theta) = k(\theta)\cdot\theta$ is given in Fig. 9.

As we can see in Figs. 8 and 9, the geometrical aspect of these hysteretic loops is different. However, the damping value is directly connected with the loop area and not with its form. Fortunately, the loop area differences are not so obvious.

This can be proved by computing the damping ratio for different amplitudes θ_0 and for each kind of hysteretic loop.

The results for different θ_0 levels of such calculus, together with the corresponding ζ experimental values, are given in Fig. 10. As we can see in this figure a reasonable accuracy for NKV model was obtained.

Therefore, we can conclude that the viscous NKV model can be used for damping evaluations of the hysteretic materials.

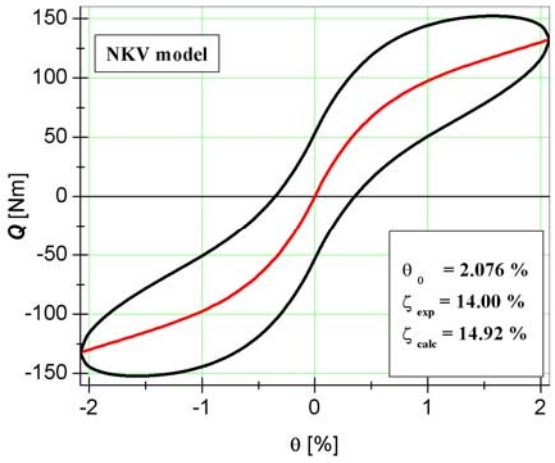

Fig. 8 NKV hysteresis loop

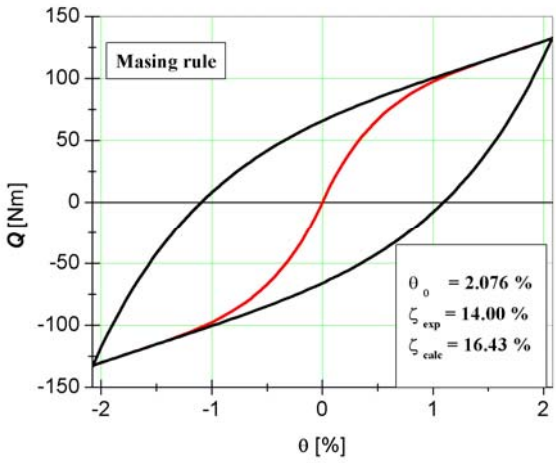

Fig. 9 Masing hysteresis loop

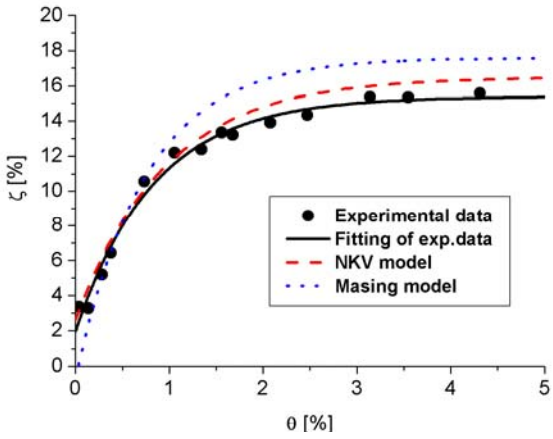

Fig. 10 Check of the damping modeling

.

4.3 Linearization

In many engineering problems the generation and solving of large nonlinear systems is not justified. Also, in structural mechanics there are efficient computational methods, based upon of the linear body hypothesis, which is correct for the structures itself but is inadequate for the materials that work together with these structures (soils for example). There is the case of base-isolated structures too. For the base-isolated structures, the linear assumption is correct for a superstructure but incorrect for an isolated layer.

This reason justifies the attempt to replace the NKV nonlinear equation (31) by an equivalent linear one:

$$\varphi'' + \tilde{c}\cdot\varphi' + \tilde{k}\cdot\varphi = \mu\cdot\sin\upsilon\tau \tag{43}$$

provided that no large difference between the non-linear and equivalent linear solutions occur.

By using a global linearization method in [5] the equivalent linear stiffness and damping coefficients $\tilde{c}$ and $\tilde{k}$ were obtained in the form:

$$\begin{aligned}\tilde{c} &= \frac{1}{\varphi_m}\int_0^{\varphi_m} c(\varphi)\cdot \mathrm{d}\varphi \\ \tilde{k} &= \frac{2}{\varphi_m^2}\int_0^{\varphi_m} k(\varphi)\cdot\varphi\cdot \mathrm{d}\varphi,\end{aligned} \tag{44}$$

where:

$$\varphi_m = \max\left|\varphi(\tau)\right| = \mu\Phi_{\max} = \frac{2\mu}{\tilde{c}\sqrt{4\tilde{k}-\tilde{c}^2}}. \tag{45}$$

Because the integration limit φ_m is function in terms of $\tilde{c}$ and $\tilde{k}$, from eqs. (44) a nonlinear system of two algebraic equations for the unknowns $\tilde{c}$ and $\tilde{k}$ is obtained.

Thus, for instance, if the material functions $c(\varphi)$ and $k(\varphi)$ have the exponential form:

$$\begin{aligned}c(\varphi) &= a_1 - a_2\cdot\exp(-a_3\varphi) \\ k(\varphi) &= b_1 + b_2\cdot\exp(-b_3\varphi),\end{aligned} \tag{46}$$

as in the tested rubber sample, by Eqs. (44) and (45) the following system follows:

$$\begin{cases} a_1\varphi_m + \dfrac{a_2}{a_3}\left[\exp(-a_3\varphi_m)\right] - \dfrac{2\mu}{\sqrt{4\tilde{k}-\tilde{c}^2}} = 0 \\ b_1\varphi_m - \dfrac{b_2}{b_3}\varphi_m\left[\exp(-b_3\varphi_m)\right] - \dfrac{4\tilde{k}\mu^2}{\tilde{c}^2\left(4\tilde{k}-\tilde{c}^2\right)} = 0 \end{cases} \tag{47}$$

This system can be numerically solved, [19] for different amplitudes μ and the equivalent linear values for $\tilde{c}$ and $\tilde{k}$ are obtained. Thus, using this method for tested rubber a set of equivalent linear constants $\tilde{c}$ and $\tilde{k}$ was obtained (Table 1) and the corresponding linearized magnification functions are given in Fig. 11.

Table 1 Equivalent linear constants

μ	$\tilde{c}$	$\tilde{k}$
10^{-4}	0.030	198
$5\cdot10^{-4}$	0.038	195
10^{-3}	0.046	188
$5\cdot10^{-3}$	0.080	154
10^{-2}	0.103	132
$5\cdot10^{-2}$	0.181	69
10^{-1}	0.205	55
$5\cdot10^{-1}$	0.225	31
1	0.227	50

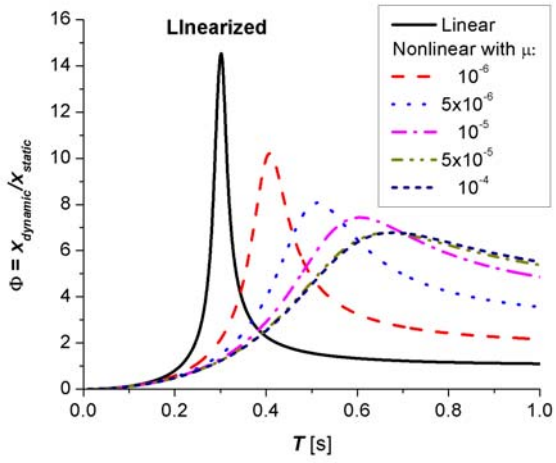

Fig. 11 Linearized magnification functions

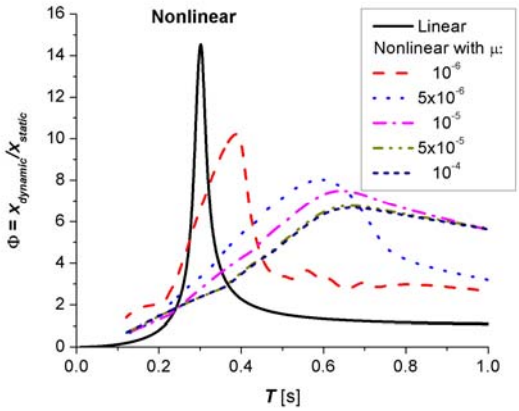

Fig. 12 Nonlinear magnification functions

The comparison between the linearized (Fig. 11) and nonlinear (Fig. 12) magnification functions shows a reasonable agreement between the shape and values of the magnification curves.

Therefore, the equivalent linear systems can satisfactorily approximate the nonlinear response.

As can see in Table 1 and Fig. 11 the equivalent linear constants $\tilde{c}$ and $\tilde{k}$ are, in fact, functions of normalized excitation amplitude μ: $\tilde{c} = \tilde{c}(\mu)$ and $\tilde{k} = \tilde{k}(\mu)$. Thus, apparently, the linearized NKV model is a nonlinear model too, containing the nonlinear characteristic functions $\tilde{c} = \tilde{c}(\mu)$ and $\tilde{k} = \tilde{k}(\mu)$ (Fig. 13).

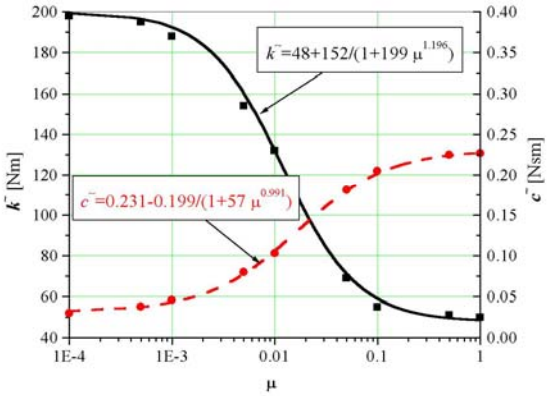

Fig. 13 Equivalent linear characteristics in terms of normalized excitation amplitude μ

However, changing the variable θ of the nonlinear problem with the new variable μ is more convenient, because θ is an unknown of the analytical solving method while the amplitude μ is not.

4 Effects of the isolator layer nonlinearity on the period-shift

Many of dissipative materials and devices used in antivibratory isolation systems exhibit a strong nonlinearity. See, for example, the result of a resonant column test performed upon rubber sample in Fig. 14 according to [6]. Using data from [13] in Fig. 15 the softening behavior of a rubber bearing isolator is illustrated. In Fig.16 we show the hardening behavior of a rubber-pendulum isolator computed with data given in [18].

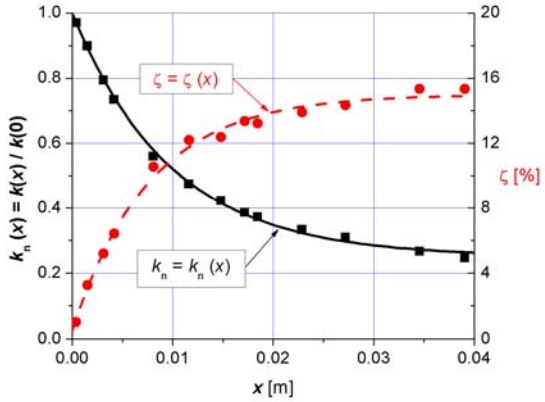

Fig. 14 Softening behavior of a rubber sample

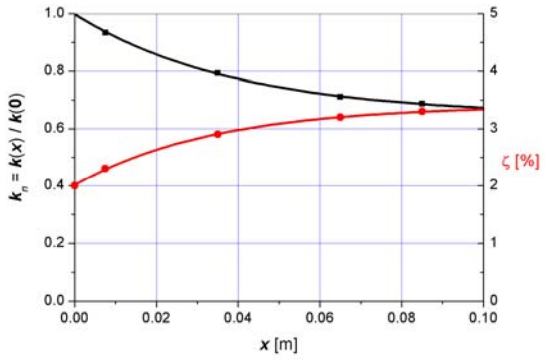

Fig. 15 Softening behavior of an LRB isolator

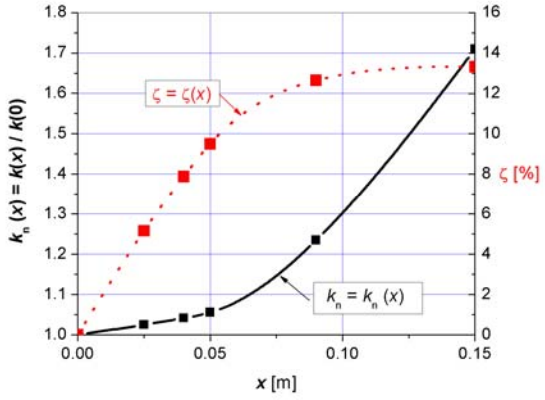

Fig. 16 Hardening behavior of an isolator

In chapter 3, a first approximation of the period-shift amount was based on the linear magnification functions, therefore on the linear behavior hypothesis for the base-isolated structure. In the example given in Fig 4, obtained by a numerical simulation, a structure was taken out from resonant conditions by a period-shift from $T_0 = 0.3$ s up to $T_0 = 0.5$ s .

To put into evidence the linear-nonlinear and softening-hardening differences, another numerical simulation study was performed using the same structure from chapter 3 but with a nonlinear isolated layer.

The nonlinear behavior was modeled by the nonlinear Kelvin-Voigt model presented in chapter 5 and the nonlinear material functions $k = k(x)$ and $c = c(x)$ were built using a test performed upon rubber (see [6]) and experimental data obtained for different isolators given in the technical literature, [1], [8], [13], [21], [25] (Fig. 18).

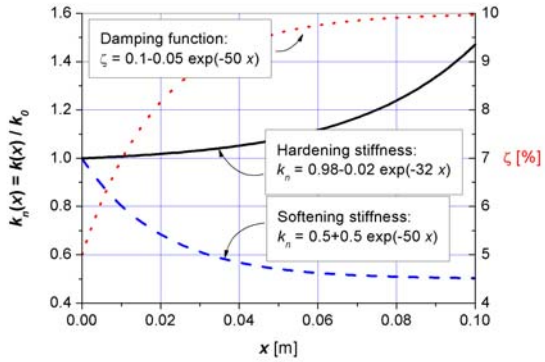

Fig.18 Nonlinear material functions used for simulations

The abutment excitation used in this simulation process was of harmonic type: $\ddot{x}_g = \ddot{x}_g^0 \sin \omega t$ with the amplitude values corresponding to peak ground acceleration observed during some earthquakes [20].

In order to compare the linear-nonlinear results and hardening-softening behavior, we used the same nonlinear damping function $\zeta = \zeta(x)$ whose initial value coincides with the 5% linear damping ratio ($\zeta_0 = \zeta(x)\big|_{x=0} = 0.05$). In addition, the initial value of stiffness functions was put in correspondence with the natural period of the isolated-base structure:

$$T_0 = 0.5\ s \Rightarrow \omega_0 = \frac{2\pi}{T_0} = 12.56 \text{ rad/s}$$

$$k_0 = m\omega_0^2 = 30,000 \times 12.56^2 = 4733 \text{ kN/m}$$

The simulation results are summarized in Fig. 19. In chapter 3, using the linear KV model, a period jump from 0.3 s to 0.5 s seems to be sufficient to take out the structure from the dangerous resonance zone. But, the nonlinear characteristics of the isolator layer change the linear period-shift estimation and can lead either to a dangerous shortening shift in the case of hardening nonlinearity or to unnecessary shift enlargement, in the case of softening nonlinearity.

This simulation proves that by neglecting the period-shift dispersion, the main purpose of the base-isolation technology (that the drawing out of structure from dangerous resonant zone) can be compromised. Also, by neglecting the nonlinear aspects, a base-isolated structure may be thrown in resonant conditions even if the structural and isolated layer natural periods are different.

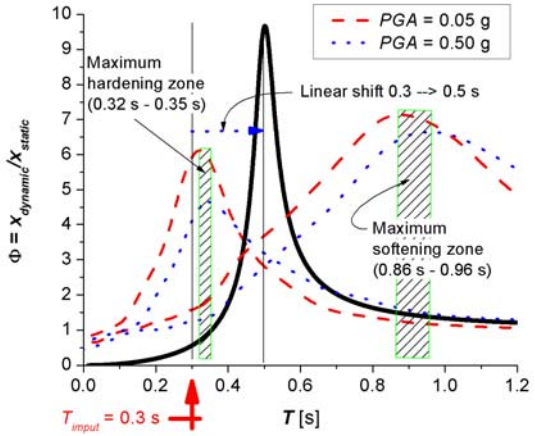

Fig. 19 Nonlinear period-shift dispersion

5 Effects of the soils nonlinearity on the period-shift

The strong dependence of the soils dynamic properties on strain or stress level produced by external loads is very well known, [4].

This nonlinear behavior is met for all site materials – more pronounced for soft degradated materials (soils) and more reduced for rocks materials.

For example, some nonlinear dynamic material functions for two extremely different site materials, one for a soft material (clay) in Fig. 20 and another for rock material (limestone) in Fig.21, are presented. Certainly, between these extremes there are a lot of site materials with an intermediary behavior.

As one can see from these experimental results, all of the site materials have the softening nonlinearity type.

Using these material functions, the nonlinear magnification functions are obtained by nonlinear

simulations, as we can see in Figs. 22 for clay, and in Fig.23 for limestone.

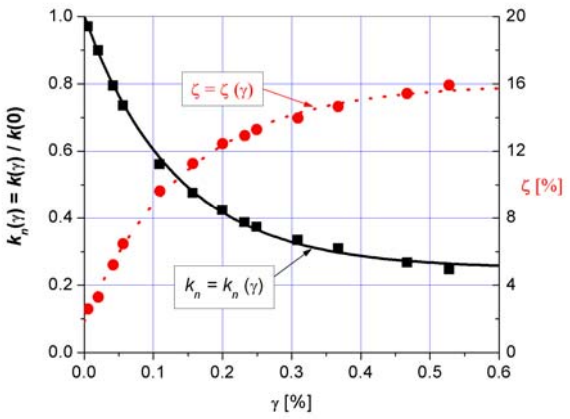

Fig. 20 Material functions for a clay sample

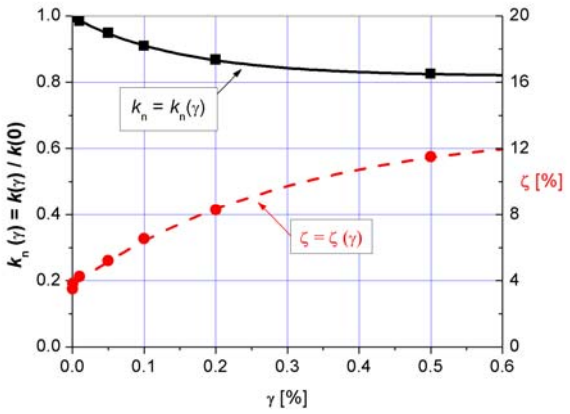

Fig. 21 Material functions for a limestone sample

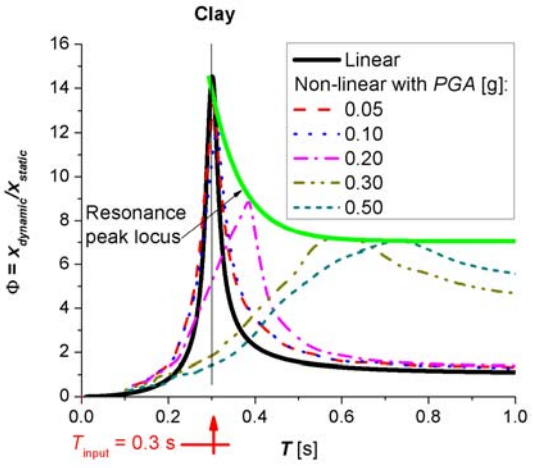

Fig. 22 Typical nonlinear magnification functions for clay

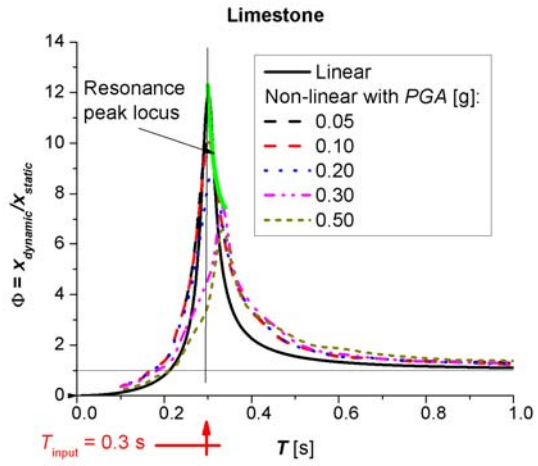

Fig. 23 Typical nonlinear magnification functions for limestone

As expected, it follows that the softening nonlinearity type of all site materials leads to the enlargement tendency of the period-shift, more pronounced at soils and more reduced at rocks.

In addition, one can remark that all these site materials have a large damping capacity.

6 Concluding remarks

- The magnification functions proved to be a proper tool for the necessary period-shift assessment.
- The period-shift from a fixed-base to an isolated base of the same superstructure depends on the nonlinear characteristics of the isolator and site layers.
- The resonant amplitude peaks of the nonlinear magnification functions are displaced towards low periods for hardening stiffness materials and towards high periods for softening stiffness materials.
- The peaks dispersion can lead to dangerous shortening or to unnecessary lengthening of the linear shift evaluation.
- The linear shift estimation must be corrected due to the nonlinear characteristics of the isolator layer and site materials.
- By neglecting the period-shift peak dispersion due to nonlinear effects and using only the linear calculus, the main purpose of the base-isolation technology (the drawing out of structure from dangerous resonant zone) can be compromised.
- In addition, by neglecting the nonlinear aspects, a base-isolated structure may be thrown in resonant conditions even if the structural and isolated layer natural periods are different.

References

[1] AIKEN I.D., Testing of seismic isolators and dampers - considerations and limitations*, Proc. Structural Engineering Congress*, San Francisco, California, July, 1998.

[2] BAJPAI V.K, GARG T.K., GUPTA M.K., Vibration-dampers for smoke stacks*, 3rd WSEAS International Conference on Applied and Theoretical Mechanics,* Spain, December 14-16, 2007, pp.124-130.

[3] BASAK S., Experimental investigation of pile group under lateral cyclic load in soft cohesiv soil*, WSEAS Transaction on Applied and Theoretical Mechanics*, 2007, pp.132-137.

[4] BRATOSIN D, A dynamic constitutive law for soils*, Proceedings of the Romanian Academy*, Vol. 3, No.1-2, 2002, pp.37-44.

[5] BRATOSIN D., SIRETEANU T., A nonlinear Kelvin-Voigt model for soils, *Proceedings of the Romanian Academy,* Vol. 3, No.3, 2002, pp.99-104.

[6] BRATOSIN D., On dynamic behavior of the antivibratory materials*, Proceedings of the Romanian Academy*, Vol. 4, No. 3, 2003, pp.205-210.

[7] BRATOSIN D., Non-linear effects in seismic base isolation*, Proceedings of the Romanian Academy*, Vol. 5, No. 3, 2004, pp.297-309.

[8] BURTSCHER S., DORFMANN A., BERGMEISTER K., Mechanical aspects of high damping rubber, *2nd Int. Symposium in Civil Engineering*, Budapest, 1998, pp.1-7.

[9] CARNEIRO J.O., DE MELLO F.J.Q., JALALI S., CAMANHO P.P., Analytical dynamic analysis of earthquake base-isolation structures using time-history superposition*, Proc. of the I MECH E Part K Journal of Multi-body Dynamics*, vol.218, no.1, 2004.

[10] DEB S.K., *Seismic base isolation - an overview,* Current Science, Vol.87, No.10, 2003, pp.1426-1430.

[11] DeSILVA, C., *Vibrations: Fundamentals and Practice,* CRC press, 2000.

[12] EHRET DOMINIK, HANNICH DIETER, SCHMITT SASCHA, HUBER GERHARD, Numerical modelling of site effects – Influences of groundwater level changes, *Proceedings of the 1st IASME / WSEAS International Conference on Geology and Seismology (GES'07)*, Portoroz, Slovenia, May 15-17, 2007, pp. 1-5.

[13] JAIN S.K., Quasi-static Testing of Laminated Rubber Bearings, *IE Journal*, Vol. 84, August 2003, pp110-115.

[14] KUNDE M.C., JANGID R.S., Seismic behavior of isolated bridges: A-state-of-art review, *Electronic Journal of Structural Engineering*, Vol. 3, 2003, pp.140-170.

[15] LEVY S., WILKINSON J.P.D., *The component element method in dynamics,* McGraw-Hill, 1976.

[16] MIRANDA C.J., Revisiting seismic isolation from a modal energy perspective, *Proceedings of the Romanian Academy*,Vol. 7, No. 1, 2006, pp.55-64.

[17] PAN Peng, ZAMFIRESCU Dan, NAKASHIMA Masayoshi, NAKAYASU Nariaki, KASHIWA Hisatoshi, Base-isolation design practice in Japan: Introduction to the post-Kobe approach, *Journal of Earthquake Engineering,* Vol. 9, No. 1, 2005, pp.147–171

[18] POCANSCHI A., PHOCAS M.C., Earthquake isolator with progressive nonlinear deformability*, Engineering Structures*, Vol. 29, 2007, pp.2586-2592.

[19] PRESS W.H., FLANNERY B.P., TEUKOLSKY S.A., VETTERLING W.T., *Numerical Recipes, The art of Scientific Computing,* Cambridge University Press, 1990

[20] RAMALLO J.C., JOHNSON E.A., SPENCER B.F., "Smart" Base Isolation Systems*, Journal of Engineering Mechanics,* Vol. 128, No. 10, 2002, pp.1088-1099.

[21] RAMORINO G., VETTURI D., CAMBIAGHI D., PEGORETTI A., ROCCO T., Developments in dynamic testing of rubber compounds: assessment of non-linear effects, *Polymer Testing*, Vol. 22, 2003, pp.681-687.

[22] SONI Ashwanijain D.K., Foundation vibration isolation method, *3nd WSEAS International Conference on Applied and Theoretical Mechanics,* Spain, December 14-16, 2007, pp. 163-167.

[23] SIRETEANU T., The effect of structural degradation on dynamic behaviour of building, *9th WSEAS International Conference on Acoustic and Music : Theory and Applications*, Bucharest, Romania, June 24-26, 2008 (in press)

[24] TSANG HING-HO, LAM NELSON T. K., ASTEN MICHAEL W., LO S. H., Generic Theoretical Formulae for Estimating Site Effects, *Proceedings of the 1st IASME / WSEAS International Conference on Geology and Seismology (GES'07)*, Portoroz, Slovenia, May 15-17, 2007, pp. 6-11.

[25] WU Yi Min, SAMALI Bilan, Shake table testing of a base isolated model, *Engineering Structures,* 24, Elsevier, 2002, pp.1203-1245.

[26] YOSIDA Junji, ABE Masato, FUJINO Yozo, Constitutive model of high-damping rubber materials*, Journal of Engineering Mechanics,* February 2004, pp.129-141.